



Effect of Hydrogen on the Properties of RF-Magnetron Sputtering ZnO:Al Films as an Alternative to Commercially Available TCO Films

Rajesh Das¹ · Himadri Sekhar Das¹

Received: 6 May 2016 / Accepted: 8 August 2016 / Published online: 1 September 2016
© The Institution of Engineers (India) 2016

Abstract Transparent conducting ZnO:Al thin films with lowest electrical resistivity and sheet resistance $3.89 \times 10^{-4} \Omega \text{ cm}$ and $7.65 \Omega/\square$ were developed by RF-magnetron sputtering using Ar + H₂ as sputtering gas at 250 °C. ZnO:Al films are highly polycrystalline hexagonal wurtzite, (002) oriented and grain size are around 30 nm. The highest carrier concentration and mobility of our lab deposited ZnO:Al films are ($\sim 10^{21} \text{ cm}^{-3}$) and $8.93 \text{ cm}^2/\text{V s}$ respectively. RF-sputtered ZnO:Al films are self textured and surface roughness of ZnO:Al films varies with H₂ dilution ratio and ultimately affects on Haze factor. Haze factor varies from 36 to 42.8 for introducing different gas ambient during deposition. Blue and green photoluminescence emission peaks are observed at 432 nm (2.87 eV) and 541.5 nm (2.29 eV) respectively in H₂ gas deposited ZnO:Al films. Both ZnO:Al and commercial TCO films have almost similar electrical properties except mobility and visible optical transmittance maxima, but still show 30 % higher optical transmittance at longer wavelength region of solar spectrum and U-type surface morphology. Systematic analysis of different materials properties, elemental analysis and surface texture of non-stoichiometric ZnO:Al films are studied and latest status on electrical, optical as well as morphological studies of magnetron sputtered ZnO:Al films are reported. Finally, the possible solutions for expected outcomes are discussed.

Keywords ZnO:Al thin film · Commercial TCO films · Magnetron sputtering · Haze factor · Figure of merit · Surface texture · H₂ gas

Introduction

Transparent conducting oxide (TCO) thin film is a special type of materials with wide band gap ($>3 \text{ eV}$), high optical transmittance ($\geq 85 \%$) over wide range of solar spectrum, and low sheet resistance.

Main important TCOs are fluorine doped tin oxide (FTO), indium tin oxide (ITO), aluminum doped zinc oxide (ZnO:Al), antimony doped tin oxide (ATO), gallium doped zinc oxide (ZnO:Ga), gallium doped indium zinc oxide (IZO:Ga), and indium doped cadmium oxide thin films. Other ternary compounds based TCO materials are Zn_2SnO_4 , MgIn_2O_4 , $\text{CdSb}_2\text{O}_6\text{:Y}$, ZnSnO_3 , GaInO , $\text{Zn}_2\text{In}_2\text{O}_5$ and $\text{In}_4\text{Sn}_3\text{O}_{12}$ etc. Among all TCO thin films fluorine doped tin oxide (FTO), and indium tin oxide (ITO) are commercially available for different device applications and the others are under lab scale development stage. TCO thin films have wide applications such as in micro-electronic devices, displays, thin film transistor, light emitting diodes (LEDs), solar cells and other photonic devices [1–6]. ZnO:Al thin films plays key role as front electrode and back reflector in thin film photovoltaic cells.

Main objective of using ZnO thin film as back reflector is to achieve enhanced light trapping in the active layer of thin film solar cell to create more numbers of photo-generated carriers that helps to improve carrier transport mechanism, ultimately to achieve stable and highly efficient solar cell. Thin ZnO layer enhances light absorption in the intrinsic layer of p–i–n structure due to multiple reflection of longer wavelength light at n-metal interface

✉ Rajesh Das
rajesh_eru2003@yahoo.com

¹ Department of Applied Sciences, Haldia Institute of Technology, Haldia 721657, West Bengal, India

and hence ultimately improves power conversion efficiency, fill factor and stability of solar cell. In that case, the series resistance of solar cell becomes very low and shunt resistance becomes infinite. To achieve the desired result, key technical specifications of ZnO thin film for solar cell applications are expected to be with ultralow sheet resistance ($<5 \Omega/\square$), higher mobility ($>100 \text{ cm}^2/\text{V s}$), almost 90 % optical transmittance throughout the entire solar spectrum and proper surface texture for 80 nm thick ZnO:Al films. Growth mechanism of RF-sputtered ZnO thin film has vital role to achieve desired electrical and optical characteristics. High defect density and voids inside ZnO films may be the cause for higher optical absorption and low carrier transport. Grain size and grain distribution in ZnO matrix can be the cause for variation of internal texture. Grain size, shape and overall grain distribution on ZnO film surface control the surface roughness which ultimately determine light scattering (diffuse and specular) and the Haze factor of TCO surface. The grain size, surface roughness, and structure of ZnO thin film are greatly affected by hydrogen plasma during ZnO film formation.

Several researchers studied the hydrogen dilution effect on electrical properties of magnetron sputtered ZnO:Al film deposited on glass substrate [7–14]. In 2004, ZnO:H film has been developed incorporating hydrogen gas during deposition and record lowest resistivity achieved to $2 \times 10^{-4} \Omega \text{ cm}$ and visible transmittance value almost 100 % deposited at 150 °C substrate temperature reported elsewhere [8]. Liu et al. [9] also achieved AZO thin film with low resistivity and high transmittance $4.15 \times 10^{-4} \Omega \text{ cm}$ and 94 % in visible range respectively by RF sputtering with Al_2O_3 of 2 wt% in Ar + H_2 ambient at 100 °C. In 2011, Zhu et al. [10] investigated the effects of hydrogen introduction during deposition and annealing on structure and optical, electrical properties of ZnO film but no significant improvement in electrical resistivity is reported. Mainly structural diversity due to thermal annealing effect is observed. Hsing et al. [11] studied on RF-magnetron sputtered AZO thin film deposited at 300 °C and effect of H_2 plasma treatment. Minimum resistivity of $1.02 \times 10^{-3} \Omega \text{ cm}$, tuning of surface roughness and surface grain size are reported. Very recently, Li et al. [12] and Chierchi et al. [14] used pulsed dc magnetron sputtering and intentionally introduced hydrogen for the development of ZnO:Al thin film with resistivity of the order of $10^{-4} \Omega \text{ cm}$ with 85 % visible transmittance in a hydrogen environment at room temperature. Record lowest resistivity of AZO thin film deposited by pulsed laser deposition technique and it is $8.54 \times 10^{-5} \Omega \text{ cm}$ [15]. But no systematic analysis on the TCO haze factor variation and tuning of surface texture for as deposited ZnO:Al film under H_2 ambient is reported.

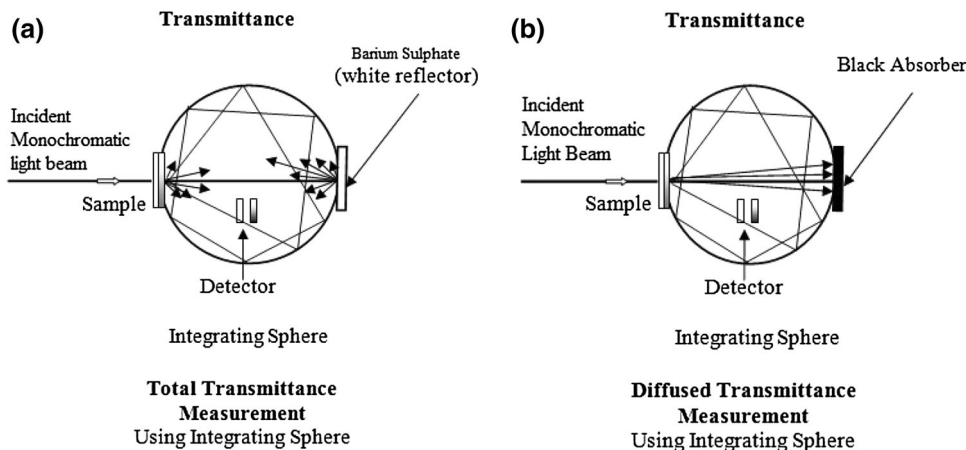
In this report, systematic studies on its size dependent electrical, optical properties (especially the diffuse transmittance, Haze factor, and photoluminescence), surface morphology of ZnO:Al films under various H_2 dilution during film growth will be reported. The achievements of ZnO:Al films as alternative TCO film will be compared with the industrial grade ITO and $\text{SnO}_2:\text{F}$ films and the state of art will be discussed.

Experimental Details

ZnO:Al thin films were deposited by dual-target RF magnetron (powered at 13.56 MHz radio frequency) sputtering system (Hind High Vacuum Co. (P) Ltd) on glass substrate at substrate temperature $T_s = 350 \text{ °C}$ under non reactive and reactive environment with Ar, Ar + O_2 and Ar + H_2 sputtering ambients. Sintered ceramic disc of Al doped ZnO (ZnO:Al 98:2 wt%) with a purity of (99.99 %) having 2 in. diameter and 5 mm thickness were used as sputtering target. The sputtering system is made of stainless steel chamber with water cooled capacitively coupled magnetron. Target material is mounted on upper holder and substrate is mounted on lower holder that has controlled rotation facility. The process chamber is evacuated up to a base vacuum of 2.6×10^{-6} torr. The RF power was varied from 50 to 90 W with a step increment of 20 W. Target to substrate distance was kept at 6 cm for all experiments. Pre-sputtering of ZnO:Al target is done in pure argon plasma atmosphere for about 10 min in order to remove the surface oxide layer of the target before deposition of the film and the glass substrates were also plasma cleaned. The modified chamber design is helpful for uniform ZnO thin film growth with high deposition rate and good adhesion with the substrate material.

The electrical properties of ZnO thin films were studied by 4-probe van-der-Pauw technique attached with Hall measurement (Ecopia-HMS-3000) set-up. Optical transmittance (specular, diffuse and total) and absorbance data of ZnO thin films were measured using microprocessor controlled UV–VIS (Perkin-Elmer Lambda-35) spectrophotometer (Integrating sphere attached). Total (Diffuse and Specular) transmittance (T_{tot}) linked with light scattering through the sample were measured using Barium Sulphate white reflector at the exit port shown in Fig. 1a. Diffuse transmittance was measured by using black absorber at the exit port, light scattering mechanism shown in Fig. 1b. Black absorber can absorb the entire specular transmittance (T_{spe}) part and hence diffuse transmittance ($T_{\text{diffuse}} = T_{\text{tot}} - T_{\text{spe}}$) was automatically measured by computer interfaced UV–VIS spectrophotometer. Finally, Haze factor (H_z) is calculated by the ratio of diffuse to total

Fig. 1 Schematic of experimental arrangement for **a** total transmittance and **b** diffuse transmittance measurement set-up of TCO thin films using integrating sphere attached with UV–VIS spectrophotometer



transmittance. For absorption measurements in the UV and optical region, the films were coated onto quartz substrates.

The photoluminescence properties of ZnO thin films were studied by PL setup with an ordinary Xenon light source using the excitation wavelength of 350 nm and the power of 150 W (Hitachi S-4500). Structural characterization of ZnO films was carried out by Crystallographic phase analysis X-ray diffraction (XRD) (Philips PW 1710 diffractometer) (Cu K_{α} , $\lambda = 1.54178 \text{ \AA}$, 2θ scan mode). The surface morphology was performed by Scanning Electron Microscopy (SEM) (Carl Zeiss SMT Supra 55). Elemental analysis was estimated by Energy dispersive X-ray spectroscopy (EDX) attached with SEM. Surface topography of ZnO films was studied by Atomic Force Microscopy (AFM) (Tap 300 G).

Results and Discussion

Initially, few sets of ZnO thin films deposition were performed with 80 W RF-power, 10 mbar chamber pressure, 250 °C substrate temperature with controlled substrate

rotation. During that time Ar flow was maintained at 40 sccm. After few runs with Ar ambient, ZnO thin films were deposited in reactive atmosphere under O_2 and H_2 gases. Especially systematic variation in H_2 concentration with Ar is done and interesting results are achieved. ZnO:Al films show promising electrical properties ($\rho = 3.79 \times 10^{-4} \text{ \Omega cm}$ and $R_{sh} = 7.65 \text{ \Omega}/\square$) due to its high carrier density but mobility is 2–3 times less compared to commercial TCO films. The details of the results, electrical properties and optical properties are shown below in Table 1. Those properties are compared with commercially available ITO and U-type $SnO_2:F$ thin films. Commercial TCO shows very low sheet resistance ($<5 \text{ \Omega}/\square$) due to both high carrier density ($\sim 10^{20} \text{ cm}^{-3}$) and mobility.

During early stages of growth, Zn atoms bind to the O-terminated surface. Free O ad-atoms or O_2 dimers aid the Zn diffusion by binding to the Zn [16]. This ad-atom cluster can then diffuse across the surface. The Zn atom then splits from the cluster when it reaches an appropriate site. Sputter deposition transfers more kinetic energy to the substrate from the higher energy impacts, hence growth is generally more complete, dense and crystalline exhibiting

Table 1 Comparative results of electrical and optical properties

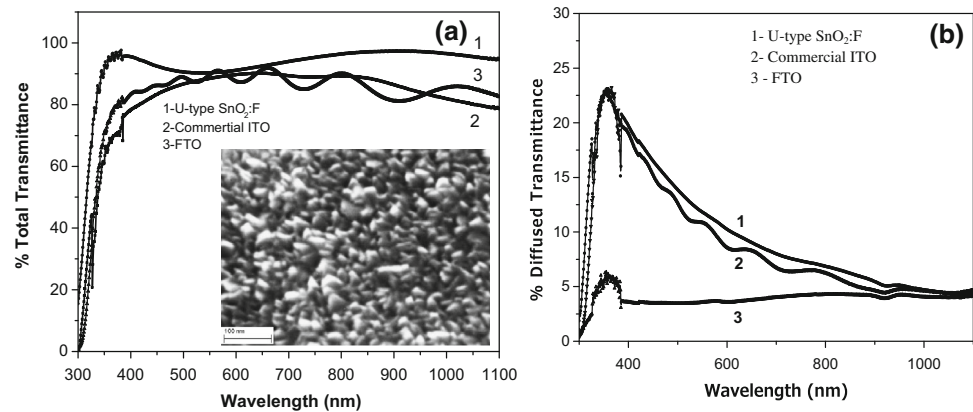
Sample	Carrier concentration (cm^{-3})	Mobility (μ) ($\text{cm}^2/V \text{ s}$)	Resistivity (ρ) (\Omega cm)	% Haze factor $H_z = (T_d/T_i) \times 100 \%$	Sheet resistance $R_{sh} = (\rho/t)$ $\text{\Omega}/\square$	Figure of merit (FOM) $\phi^{TC} = T^{10}/R_{sh}$
Commercial $SnO_2:F$	7.35×10^{20}	18.37	2.78×10^{-4}	7	4.63	1.50×10^{19}
Commercial ITO	1.73×10^{21}	11.58	3.12×10^{-4}	25	5.2	6.70×10^{18}
ZnO:Al	7.56×10^{20}	1.92	4.30×10^{-3}	36	67.5	5.2×10^{17}
Ar deposited						
ZnO:Al	3.54×10^{20}	3.28	5.37×10^{-3}	42.8	80	4.4×10^{17}
Ar + O_2						
ZnO:Al	1.80×10^{21}	8.93	3.89×10^{-4}	41.2	7.65	4.76×10^{18}
Ar + H_2 ($C_H = 5 \%$)						

Table 2 Elemental analysis of ZnO:Al films deposited under Ar + H₂ ambients with different concentration ratio

Elements	Composition (wt%) and stoichiometry for ZnO:Al films			
	C _H = 5 %	C _H = 10 %	C _H = 20 %	C _H = 40 %
O K	24.65 ± 0.57	24.24 ± 0.53	24.20 ± 0.53	23.87 ± 0.52
Al K	1.38 ± 0.13	1.51 ± 0.14	1.22 ± 0.14	1.04 ± 0.13
Zn L	73.97 ± 0.51	74.35 ± 0.54	74.58 ± 0.53	75.09 ± 0.53
Stoichiometry	Zn _{1.13} O _{1.54} :Al _{0.051}	Zn _{1.14} O _{1.51} :Al _{0.056}	Zn _{1.14} O _{1.51} :Al _{0.045}	Zn _{1.15} O _{1.49} :Al _{0.038}
PL-peak position (eV)	2.65	2.79	2.29, 2.65, 2.87	No data

Table 3 Variation of H₂ flow dependent electrical resistivity, carrier concentration and mobility of Ar + H₂ deposited ZnO:Al thin films

No. of obs.	H ₂ flow (%)	Resistivity (Ω cm)	Carrier concentration (cm ⁻³)	Mobility (cm ² /V s)	Sheet resistance (Ω/□)	FOM $\phi^{TC} = T^{10}/R_{sh}$
1.	5	3.89×10^{-4}	1.8×10^{21}	8.93	7.65	4.76×10^{18}
2.	10	8.6×10^{-4}	9.8×10^{20}	7.5	30.7	1.06×10^{18}
3.	20	9.1×10^{-3}	1.9×10^{20}	3.6	126.7	3.9×10^{17}

Fig. 2 Comparative optical properties (total and diffuse transmission spectra) of both for commercial TCO films (*inset* SEM image for U-type SnO₂:F film)

less stacking faults. Under Ar + H₂ plasma, the growth mechanism of non-stoichiometric ZnO:Al films are something complex, the growth mode can produce incoherent grain boundaries, high density of threading dislocations and stacking faults. ZnO films growth under excessive H₂ dilution oxygen deficient zinc-blende phase are formed instead of wurtzite structure. O-deficient or Zn rich films are formed, Zn²⁺ ion will be replaced by Al³⁺ ions or Zn–H bond can be formed that contributes in enhancement in free carrier density [17, 18] ultimately increases electrical conductivity of ZnO:Al films. In hexagonal closed packed arrangement, grain boundary scattering increases, that may be the cause for lower value of mobility in ZnO:Al films. Elemental analysis of ZnO:Al films and the systematic variation of electrical properties deposited under Ar + H₂ ambients with different C_H values are shown in Tables 2 and 3 respectively.

Figure 2a, b shows the comparative optical properties (total and diffuse transmission spectra) of commercial

TCO. Commercial TCO films show high optical transmission (90 %) over wide range of wavelength in solar spectrum, and tunable Haze factor starting from 7 % to maximum 25 %. Figure 3 shows the variation of total and diffuse optical transmission of ZnO:Al films deposited under various C_H ratio. RF-sputtered ZnO:Al films show almost 90 % visible transmission but in higher wavelength (at 1100 nm) %T becomes 60 %, and also significant amount UV-absorption loss are observed in ZnO:Al films. But in the present study the role of different sputtering gas to control the haze factor of as deposited ZnO:Al films are reported (shown in Table 1). Especially effect of hydrogen on ZnO:Al films properties are reported in this article. Non-stoichiometric ZnO:Al films show Haze factor starting from 36 % to maximum 42 % under Ar + H₂ ambient. Selected groups reported about systematic analysis of controlling Haze factor of ZnO:Al thin film based alternative TCO development and it is done by either wet chemical etching or by plasma etching [19–21]. The small-

Fig. 3 Comparative optical transmittance ZnO:Al films **a** total optical transmittance of Ar + H₂ deposited ZnO:Al films under different hydrogen dilution (*inset* SEM image for best ZnO:Al film), **b** comparative diffuse optical transmittance under different gas ambient, **c** variation of Haze factor of ZnO:Al films with the variation of C_H values

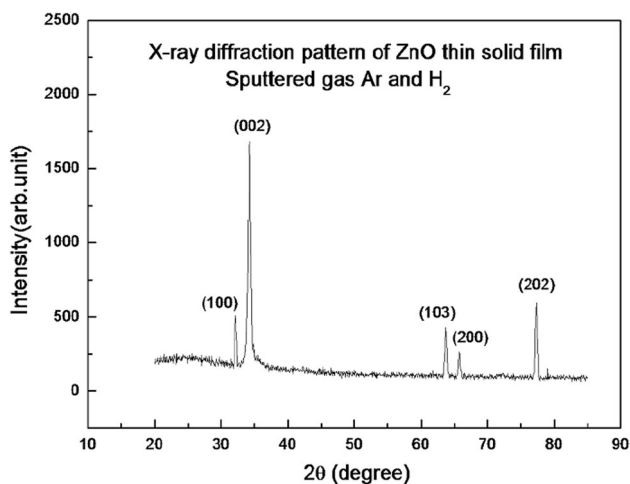
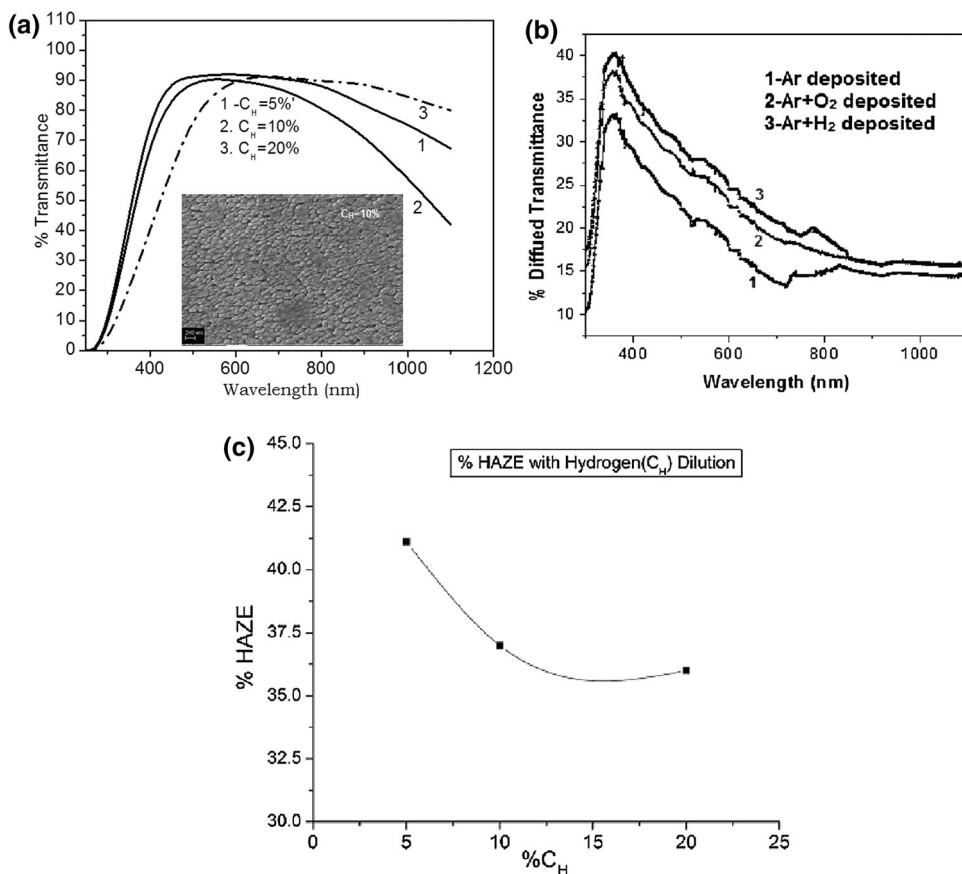


Fig. 4 XRD spectrum of ZnO:Al film deposited under Ar + H₂ ambient

scale structure of ZnO thin film materials in terms of geometrical shape, distribution of size, describes the optical response of the nano-structured materials. Sputtering ambients have an important role to control the surface morphology, structure, grain size distribution as well as optical properties. The variation of hydrogen concentration

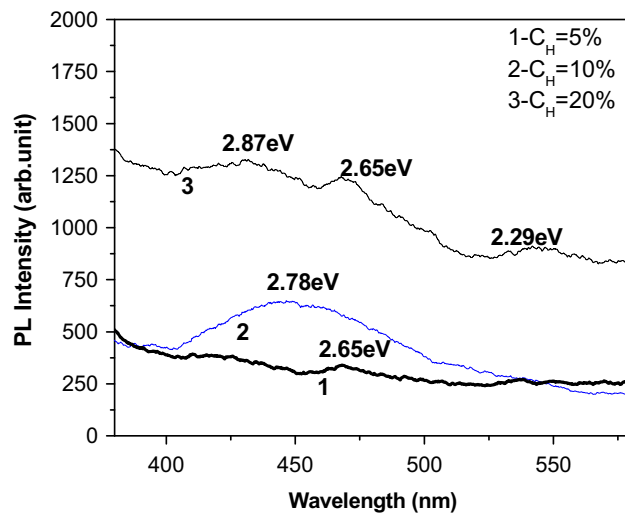


Fig. 5 PL spectra of ZnO:Al films **a** ZnO:Al (C_H = 5 %), **b** ZnO:Al (C_H = 10 %) and **c** ZnO:Al (C_H = 20 %)

C_H (C_H = H₂/(Ar + H₂) × 100 %) in plasma atmosphere has significant role on the grain size variation and surface texture of as deposited ZnO thin film and it is highly correlated with variation of haze factor with decrease of grain size. Variation of Haze factor of ZnO:Al films with the variation of C_H values during film deposition is shown in

Fig. 3c. It is observed that with increase of hydrogen concentration in vacuum chamber during deposition Haze factor initially decreases and finally saturates. As the hydrogen dilution increases deposition rate also decreases. Diffused transmittances decrease with increase in hydrogen concentration grain size decreases. As a result diffused transmittance decreases and finally sharp decreases of Haze

factor of Ar + H₂ deposited ZnO:Al films are observed. Details of scattering mechanism from rough TCO surface, agreement of theoretical prediction with experimental measurement of Haze factor has been discussed by Jäger and Zeman [22]. Excessive increase of H-dilution in sputtering gas ambient may cause for increase of amorphous region and void can be increased in ZnO:Al matrix,

Fig. 6 2d- and 3d-topography of Atomic force microscopy (AFM) **a** SnO₂:F-U-type, **b** ZnO:Al (C_o = 2 %), and **c** ZnO:Al (C_H = 10 %)

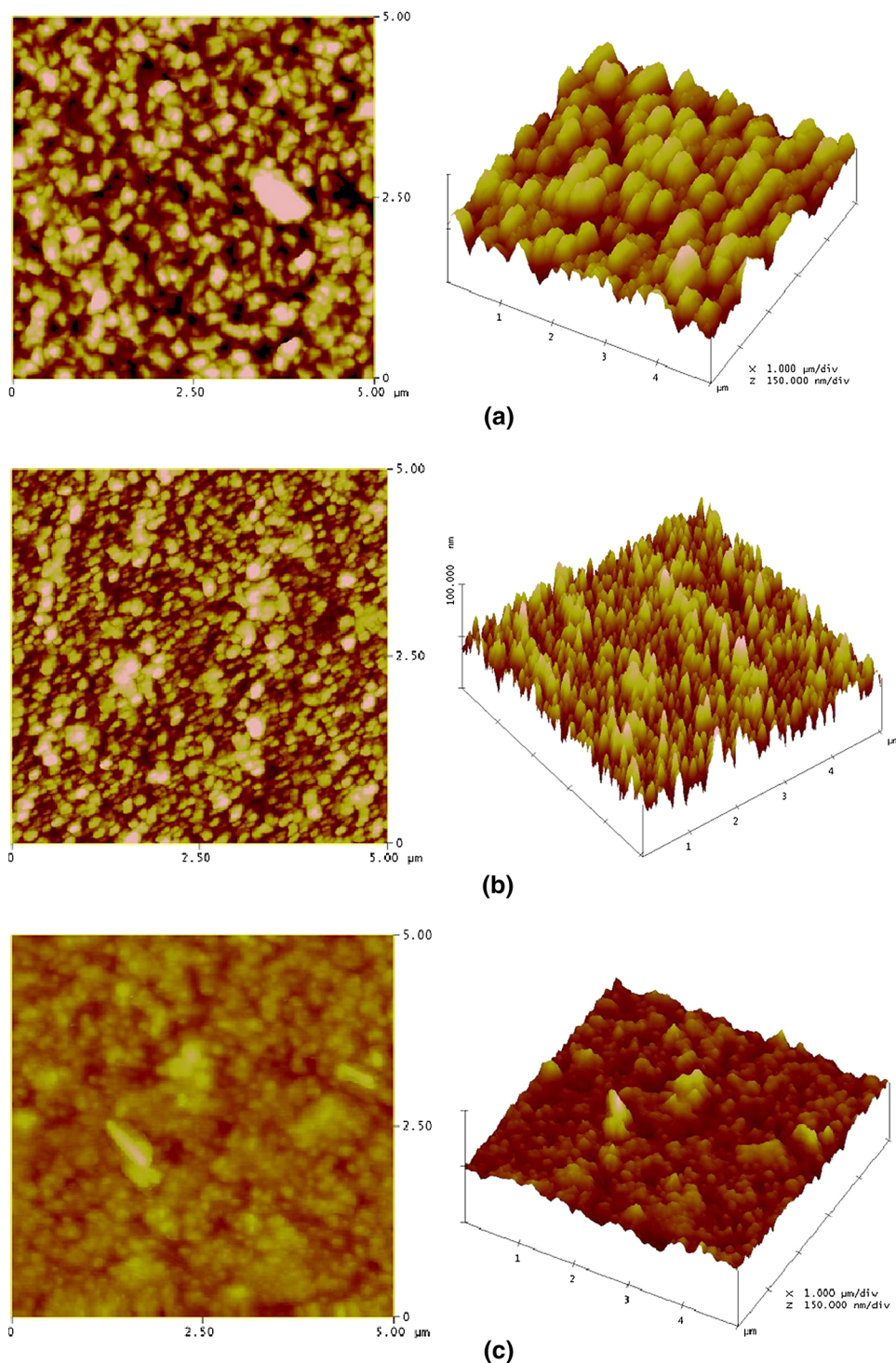


Table 4 Variation of optical transmission, and bandgap energy of ZnO films with different hydrogen gas concentration ratio during deposition

C_H value	Electrical sheet resistance (Ω/\square)	% Optical transmittance (%T) at			Grain size (nm)	Surface roughness (nm)	Grain distribution	Optical bandgap E_g (eV)
		400 nm	700 nm	1100 nm				
5	7.65	70	90.4	65.4	19	8.355	Granular, oval and round shape	3.62
10	30.7	69.5	89.4	32.3	15	9.962	Granular and round shape	3.82
20	126.7	35	93.3	81.9	22	19.603	Rhombohedral	3.56

ultimately absorption increases in longer wavelength region. Under Ar + H₂ ambient with $C_H = 10\%$, ZnO film surface are etched and the surface morphology consists of large number of pores.

Figure 4 shows the XRD spectrum of rf-magnetron sputtered ZnO:Al films deposited under Ar + H₂ ambient in optimum deposition. For polycrystalline sample, crystallites are randomly oriented, but for sputtered ZnO thin film, X-ray diffraction pattern shows preferred (002) orientation of ZnO crystallites, it is hexagonal, wurtzite and c-axis orientation (perpendicular to substrate). Crystallite sizes are estimated by Scherrer's formula. During non-reactive sputtering, Zn and O atoms rarely combine in Ar plasma environment, arriving often as single Zn or O species onto the substrate. But under reducing atmosphere (deposited with $C_H = 10\%$) polycrystalline ZnO thin films are formed with alternating planes of tetrahedrally coordinated O²⁻ and Zn²⁺ stacked along the c-axis. Initially at $T_s = 350\text{ }^\circ\text{C}$ substrate has an O vacancy, which causes some point defects. The first new layer exhibits a large O-deficiency, along with a highly mismatched phase structure. The high defect density, coupled with the O-deficiency has allowed the formation of a phase boundary between the wurtzite and zinc blende phases. But, in reactive environment with Ar + H₂ plasma, higher O deficient non-stoichiometric highly mismatched ZnO:Al films with many defects are formed. Replacement of Zn²⁺ by Al³⁺ or Zn–H bond formation can create lattice misfits and lattice strain. Vacancy clustering and ordering may hamper film properties in hexagonal structure of ZnO:Al films. Zn–O bond length is 1.9767 Å and Zn–H bond length is 1.535 Å. Also, during ZnO:Al film formation Al³⁺ can easily replace of Zn²⁺ in lattice due to its smaller ionic radius of Al³⁺ (0.54 Å) than that of Zn²⁺ (0.74 Å) [23–26], leading to a reduction of the lattice parameter and ultimately forms reduced grain structure.

Figure 5 shows the photoluminescence peak of non-stoichiometric ZnO:Al thin films at 2.29, 2.65 and 2.78 eV deposited under Ar + H₂ ambient with different hydrogen dilution. Different optical transitions are due to o-vacancy (blue emission) and green emission is due to Zn vacancy. 2.65 and 2.78 eV two emission peaks are basically two blue emission peaks corresponding two 468

and 444 nm respectively. Blue and green photoluminescence (PL) emission peaks are observed at 432 nm (2.87 eV) and 541.5 nm (2.29 eV) respectively in H₂ gas deposited ZnO:Al films. The green emissions may be attributed to the transition from conduction band bottom to the antisite O_{Zn} level formed in the band gap. Here, "O_{Zn}" means antisite defects, i.e., it denotes the improper localization (or) placement of oxygen atoms in the place of zinc atoms.

Figure 6 a–c shows 2d- and 3d-view of AFM-images for the evaluation of the surface topography and morphology of Commercial SnO₂:F and different ZnO:Al films. Figure 6a shows the Tetragonal phase and U-type surface profile of SnO₂:F film (2d- and 3d-view of AFM image). Pyramidal structure type morphology of U-type Fluorine doped tin oxide (FTO) deposited by atmospheric pressure chemical vapour deposition is reported by Sato et al. [27]. The surface of ZnO film deposited under Ar + O₂ ambients becomes significantly textured shown in Fig. 6b. Nanocrystallites are formed, and rough surface is achieved under high O₂ ambients. Figure 6c shows nanotextured surface features in Ar + H₂ deposited ($C_H = 5\%$) ZnO:Al film where granular-oval and round shape morphology is observed. Here the root mean square roughness and height function are used to describe the surface morphology of rough surface. Details of surface roughness variation due to the effect of hydrogen ambient are enlisted in the Table 4.

Conclusions

ZnO:Al films are deposited with Ar, Ar + O₂, and Ar + H₂ ambients. Systematic studies on electrical, optical (both total and diffuse) transmittance, Haze factor etc. of ZnO:Al films are reported. Transparent conducting ZnO:Al film with minimum resistivity = $3.89 \times 10^{-4}\ \Omega\ \text{cm}$, lowest sheet resistance = 7.65 Ω/\square and % visible transmittance ~ 90 % is developed. Sputtered ZnO:Al films are self surface textured, surface roughness of ZnO:Al film varies from 8.355 to 19.6 nm and haze factor varies from 36.2 to 42.2 with the variation of sputtering gas ambient. Commercial TCOs show controlled haze factor and it is 25 for ITO and lowest value is 7 for U-type SnO₂:F films.

Haze factor for ZnO:Al films are tuneable. As deposited ZnO:Al films show different surface topography under different H₂ dilution and maximum values of its Haze factor are sufficiently higher.

Acknowledgments The authors acknowledge Department of Science and Technology, Govt. of India [DST/TM/SERI/2K10/67(G)] for financial support for pursuing the R&D activity.

References

- J. Rodríguez-Báez, A. Maldonado, G. Torres-Delgado, R. Castanedo-Pérez, M. dela, L. Olvera, *Mater. Lett.* **60**, 1594 (2006)
- H. Gomeza, A. Maldonado, M.D.L.L. Olvera, D.R. Acosta, *Sol. Energy Mater. Sol. Cell* **87**, 107 (2005)
- Z. Liu, E. Lei, J. Ya, Y. Xin, *Appl. Surf. Sci.* **255**, 6415 (2009)
- M.A. Lucio Lopez, M.A. Luna Arias, A. Maldonado, M.D.L.L. Olvera, Acosta, *Sol. Energy Mater. Sol. Cell* **90**, 733 (2006)
- R. Martins, R. Igreja, I. Ferreira, A. Marques, A. Pimentel, A. Gonçalves, E. Fortunato, *Mater. Sci. Eng. B* **118**, 135 (2005)
- P.P. Sahay, R.K. Nath, *Actuator B* **133**, 222 (2008)
- M.L. Addonizio, A. Antonaia, G. Cantele, C. Privato, *Thin Solid Films* **349**, 93 (1999)
- L.Y. Chen, W.H. Chen, J.J. Wang, F.C.N. Hong, *Appl. Phys. Lett.* **85**(23), 5628 (2004)
- W.F. Liu, G.T. Du, Y.F. Sun, J.M. Bian, Y. Cheng, T.P. Yang, Y.C. Chang, Y.B. Xu, *Appl. Surf. Sci.* **253**, 2999 (2007)
- B.L. Zhu, J. Wang, S.J. Zhu, J. Wu, R. Wu, D.W. Zeng, C.S. Xie, *Thin Solid Films* **519**, 3809 (2011)
- F.H. Wang, H.P. Chang, C.C. Tseng, C.C. Huang, *Surf. Coat. Technol.* **205**, 5269 (2011)
- M.C. Li, C.C. Kuo, S.H. Peng, S.H. Chen, C.C. Lee, *Appl. Opt.* **50**(9), C197 (2011)
- H.B. Zhou, H.Y. Zhang, Z.G. Wang, M.L. Tan, *Mater. Lett.* **74**, 96 (2012)
- R. Chierchi, E. Salza, A. Mittiga, *Energy Proc.* **60**, 135 (2014)
- H. Agura, A. Suzuki, T. Matsushita, T. Aoki, M. Okuda, *Thin Solid Films* **445**, 263 (2003)
- S. Blackwell, R. Smith, S.D. Kenny, J.M. Walls, C.F. Sanz Navarro, *J. Phys. Condens. Matter* **25**(13), 135002 (2013)
- R. Das, K. Adhikary, S. Ray, *Jpn. J. Appl. Phys.* **47**, 1501 (2008)
- W.W. Wanga, X.G. Diaoa, Z. Wanga, M. Yanga, Z. Wub, *Thin Solid Films* **491**, 54 (2005)
- F.H. Wang, H.P. Chang, C.C. Tseng, C.C. Huang, H.W. Liu, *Curr. Appl. Phys.* **11**, S12 (2011)
- F.H. Wang, H.P. Chang, C.C. Tseng, C.C. Huang, *Surf. Coat. Technol.* **205**, 5269 (2011)
- X. Yan, S. Venkataraj, A.G. Aberle, *Int. J. Photoenergy* **2015**, 548984 (2015)
- K. Jäger, M. Zeman, *Appl. Phys. Lett.* **95**, 171108 (2009)
- J. Jie, G. Wang, X. Han, Q. Yu, Y. Lia, G. Li, J.G. Hou, *Chem. Phys. Lett.* **387**, 466 (2004)
- C. David, T. Girardeau, F. Paumier, D. Eyidi, B. Lacroix, N. Papathanasiou, B.P. Tinkham, P. Guérin, M. Marteau, *J. Phys. Condens. Matter* **23**, 334209 (2011)
- S.Y. Bae, C.W. Na, J.H. Kang, J. Park, *J. Phys. Chem. B* **109**, 2526 (2005)
- A.K.K. Kyaw, X.W. Sun, J.L. Zhao, J.X. Wang, D.W. Zhao, X.F. Wei, X.W. Liu, H.V. Demir, T. Wu, *Appl. Phys.* **44**, 045102 (2011)
- K. Sato, Y. Gotoh, Y. Wakayama, Y. Hayashi, K. Adachi, N. Nishimura, *Rep. Res. Lab. Asahi Glass Co. Ltd.* **42**, 129 (1992)